

Incorporation of an Extended Kalman Filter into the FMDSMAA Algorithm

The Forward Modeling/Downhole Simplex Method Absorption Analysis (*FMDSMAA*) algorithm takes into account the source wave’s true raypath, geometric spreading, apparent attenuation (refraction at an interface) and material losses (absorption). The *FMDSMAA* algorithm also addresses limitations of the spectral ratio technique such as inaccurate raypath assumptions and significant spectral ratio estimation sensitivities¹.

An essential part of the *FMDSMAA* implementation is to identify seismic traces with either poor trace metrics or nonsensical Peak Particle Accelerations (PPAs) indicative of a nonconstant source energy output (e.g., plate slippage, poor trace quality and/or poor or variable hammer impacts). The *FMDSMAA* algorithm was initially implemented where traces were iteratively dropped due to large *FMDSMAA* residually errors².

To address this requirement BCE has developed a new algorithm which incorporates an Extended Kalman Filter (EKF) into the *FMDSMAA* algorithm. The EKF applies a multicomponent exponential best fit to all the measured and normalized PPAs of a DST profile. This is similar to BCE’s *DSTPolyKF* algorithm for best fitting arrival time data sets with high order polynomials³. In the EKF case the best fit function is required to be a decreasing function (i.e., amplitude generally decreases with depth⁴). The EKF incorporated into the *FMDSMAA* algorithm is referred to as the *EKFAE* (EKF Amplitude Estimation). The *EKFAE* best fit function is outlined below:

$$f(d) = \sum_{i=1}^N e^{-d|\alpha_i|} \quad (1)$$

d is the depth and parameters α_i ($i = 1$ to N) are to be estimated with an EKF.

An EKF is implemented for estimating parameters α_i ($i = 1$ to N) since the measurement equation outlined in eq. (1) is nonlinear. The full details of the *EKFAE* corresponding governing equations will shortly be submitted for publication. This technical note outlines the impressive results obtained from implementing the *EKFAE* and *FMDSMAA* algorithms on a real DST data set. Figure 1 illustrates the filtered (200Hz low pass) X(t) and Y(t) component DST time series for SH source wave data acquired on the right side of the seismic sensor. The source wave data was generated with a constant output energy pendulum impact source. Figure 2 illustrated the corresponding SH full wave ($|\rho(t)| = \sqrt{(X(t))^2 + (Y(t))^2}$) time series with associated PPAs displayed. Table 1 outlines the estimated arrival times and normalized PPAs for the traces illustrated in Fig 2. Table 1 also outlined the approximated soil densities (assumed constant for this analysis). It is clear from Table 1 that the measured amplitudes have numerous inconsistencies (e.g., amplitude at 5.35m is

¹ https://users.neo.registeredsite.com/1/4/2/21752241/assets/Baziw_Verbeek_DFI_Conference_Paper_2019.pdf

² <https://users.neo.registeredsite.com/1/4/2/21752241/assets/ISC2020-139.pdf>

³ https://users.neo.registeredsite.com/1/4/2/21752241/assets/Baziw_Verbeek_DFI_Conference_Paper_2022.pdf

⁴ https://www.bcengineers.com/assets/BCE_Technical_Note_37.pdf

significantly greater than amplitude at 4.35m) and it would have been very difficult to obtain absorption estimates only using the measured values.

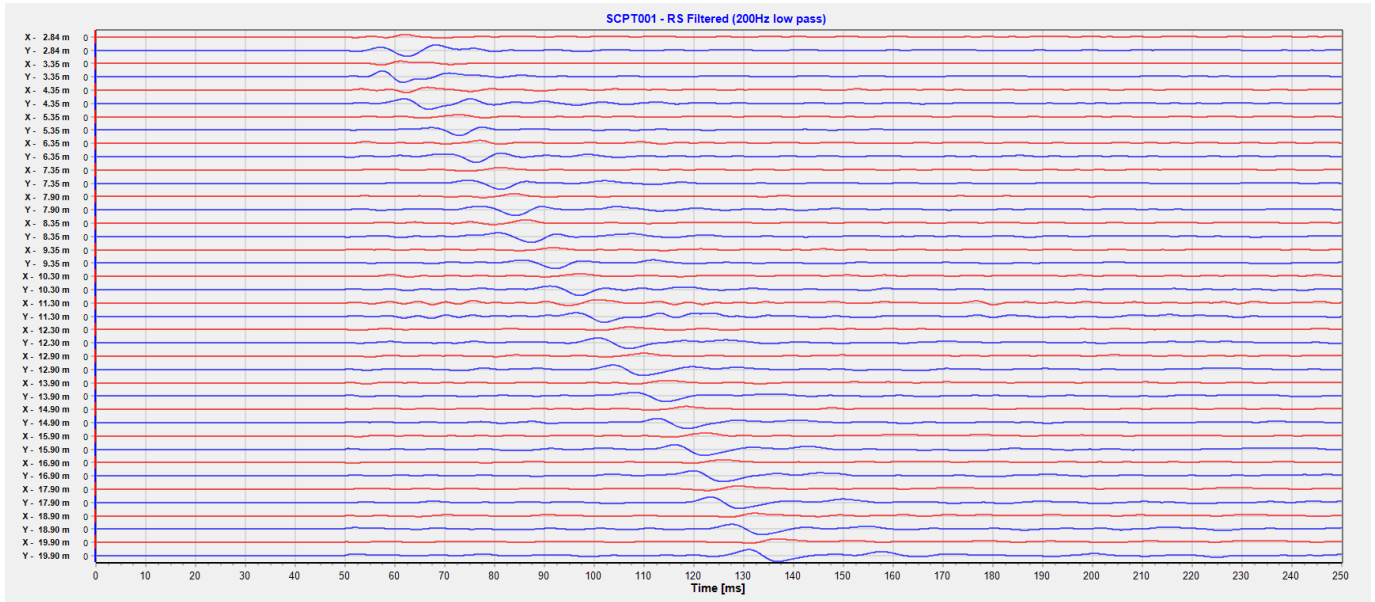


Figure 1. Filtered X and Y axis DST data acquired with a constant energy output pendulum SH source.

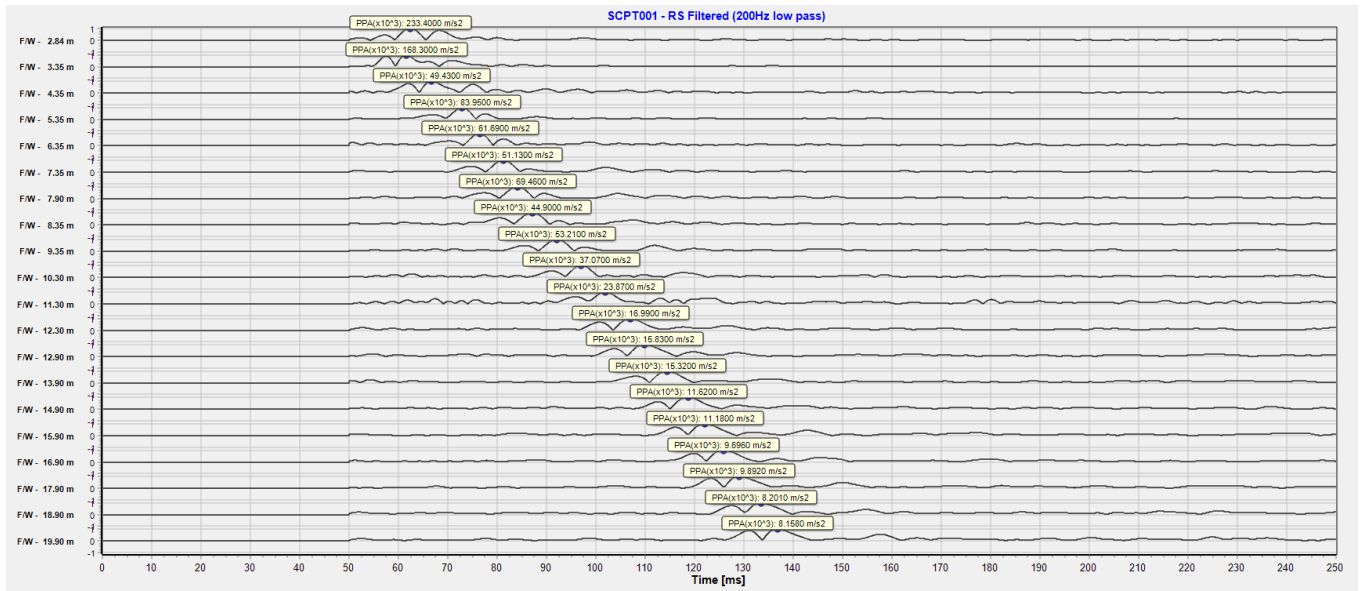


Figure 2. Full waveforms and PPAs for traces illustrated in Fig. 1

Table 1. Arrival times, PPAs and densities for trace illustrated in Fig 2.

Depth [m]	Right Arrival Time [ms]	Amplitudes [normalized]	Densities [kg/m ³]
2.84	55.1992	1	1750
3.35	55	0.720629	1750
4.35	60.1693	0.210455	1750
5.35	66.2548	0.359737	1750
6.35	69.6213	0.26404	1750
7.35	74.6013	0.218869	1750
7.9	77.5396	0.296992	1750
8.35	80.7168	0.191605	1750
9.35	85.5076	0.227291	1750
10.3	90.4079	0.157911	1750
11.3	95.3581	0.101389	1750
12.3	100.3779	0.07224	1750
12.9	103.1369	0.067148	1750
13.9	107.7085	0.064979	1750
14.9	112.081	0.049337	1750
15.9	115.4275	0.047234	1750
16.9	119.1725	0.040887	1750
17.9	122.4693	0.04158	1750
18.9	126.9911	0.034661	1750
19.9	130.258	0.034206	1750

and *EKFAE* normalized PPAs for a 0.5m depth increment.

Figure 3 illustrates a *DSTPolyKF* algorithm 6th order polynomial (blue line) best fit (0.5m resolution) for the arrival times (red dots) outlined in Table 1. Figure 4 illustrates the *EKFAE* (blue line) best fit (0.5m resolution) for the normalized amplitudes (red dots) outlined in Table 1. Parameter *N* in eq. (1) was set to 8 and two sets of estimates were obtained for depth intervals 2.84m to 11.3m and 11.3m to 19.9m. Figure 5 illustrates the corresponding *EFKAE* estimated exponential functions for depth interval 2.84m to 11.3m.

Figure 6 illustrates the estimated *FMDSM* interval velocities after processing the *DSTPolyKF* 6th order polynomial arrival time estimates illustrated in Fig. 3. Table 2 outlines the estimated *DSTPolyKF* arrival times, associated *FMDSM* interval velocities and *EKFAE* normalized PPAs for a 0.5m depth increment.

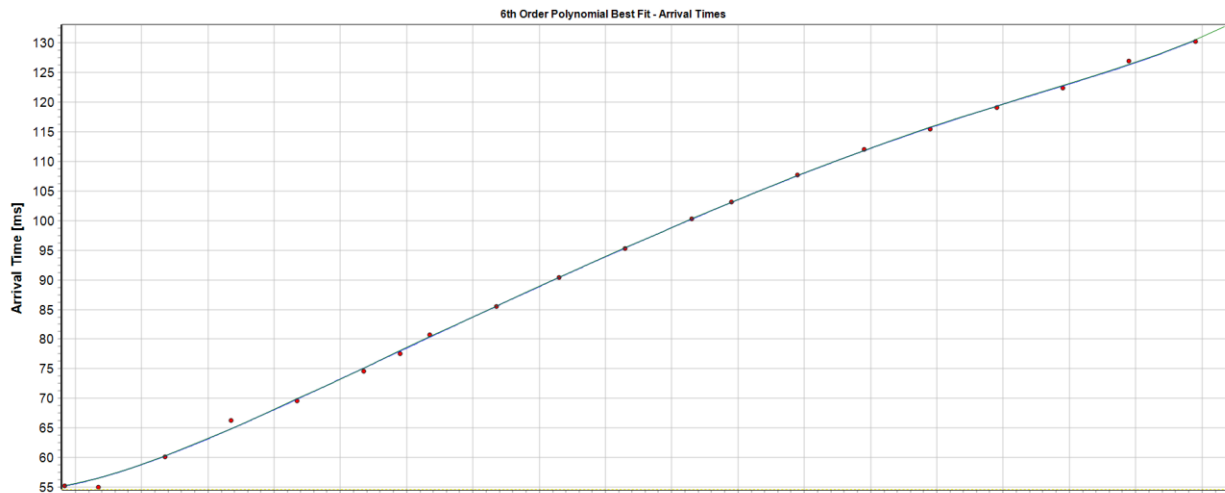


Figure 3. *DSTPolyKF* 6th order polynomial (blue line) best fit (0.5m resolution) for the arrival times (red dots) outlined in Table 1.

Figure 7 illustrates the estimated *FMDSMAA* quality factor (Q) values after inputting the *DSTPolyKF*, *FMDSM* and *EKFAE* estimates outlined in Table 2. Table 3 outlines the corresponding *FMDSMAA* estimates of absorption (α), Q , damping ratio ($\eta = 1/2Q$), wavelength (λ) and amplitude ratio residual. As is evident from Table 3, the estimated values have low associated error residuals. In addition, the estimated *FMDSMAA* values are consistent with field measurements for soils as outlined by Table 4.

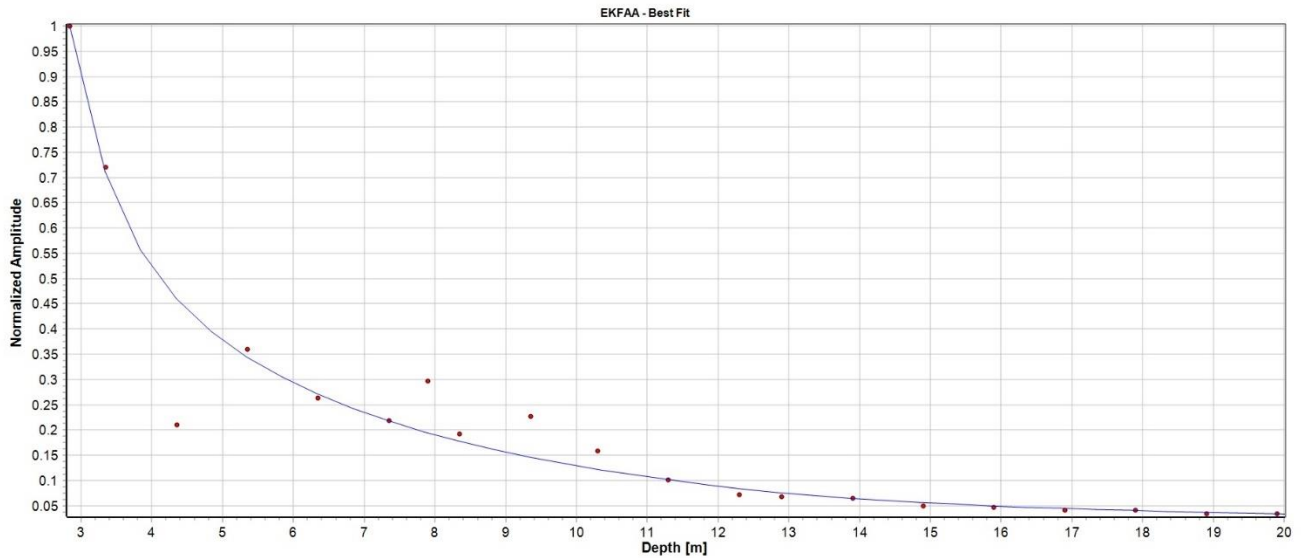


Figure 4. EKFAE (blue line) best fit (0.5m resolution) for the normalized amplitudes (red dots) outlined in Table 1.

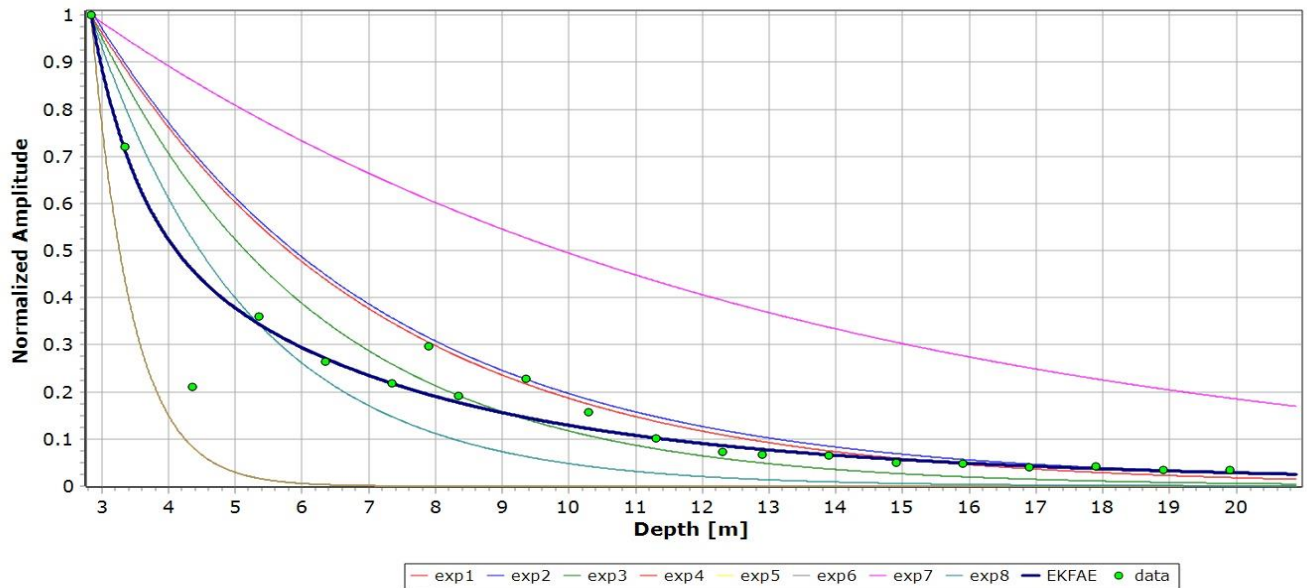


Figure 5. EKFAE (blue line) best fit (0.5m resolution) and corresponding estimated exponential functions.

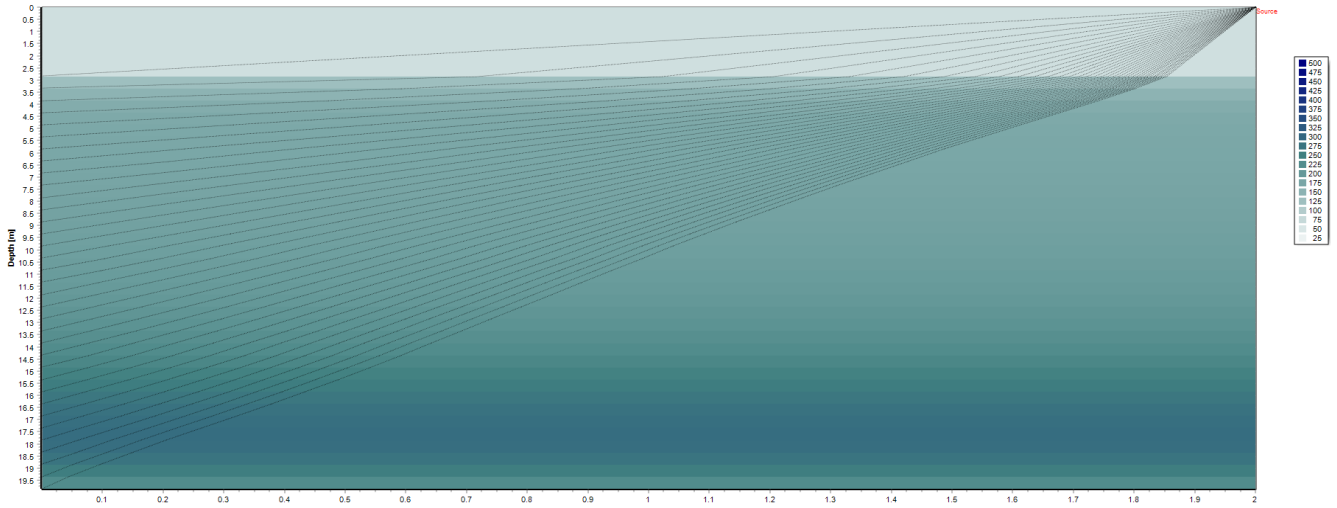


Figure 6. Estimated *FMDSM* interval velocities after processing the *DSTPolyKF* 6th order polynomial arrival time estimates illustrated in Fig. 3.

Table 2. Estimated *DSTPolyKF* arrival times, *FMDSM* interval velocities and normalized PPAs.

Depth [m]	Right Arrival Time [ms]	Right Interval FMDSM Velocity [m/s]	Amplitudes [normalized]	Densities [kg/m ³]
2.84	55.1992	62.9	1	1750
3.34	56.53352	126.5	0.718948	1750
3.84	58.23894	149.4	0.565542	1750
4.34	60.24108	162.4	0.468318	1750
4.84	62.46214	168.5	0.400462	1750
5.34	64.83991	171.2	0.349609	1750
5.84	67.32552	172.5	0.309467	1750
6.34	69.88131	173.6	0.276539	1750
6.84	72.4789	174.9	0.248738	1750
7.34	75.09741	176.5	0.224753	1750
7.84	77.72187	178.3	0.203728	1750
8.34	80.34175	180.4	0.185079	1750
8.84	82.94977	182.6	0.168397	1750
9.34	85.54072	184.9	0.153384	1750
9.84	88.11061	187.3	0.139815	1750
10.34	90.65587	189.9	0.127513	1750
10.84	93.17278	192.6	0.116337	1750
11.34	95.65707	195.7	0.106169	1750
11.84	98.10367	199.2	0.096907	1750
12.34	100.5066	203.2	0.088466	1750
12.84	102.8591	207.8	0.080768	1750
13.34	105.1539	213.3	0.073746	1750
13.84	107.3837	219.8	0.067339	1750
14.34	109.5416	227.3	0.061491	1750
14.84	111.6221	235.9	0.056154	1750
15.34	113.6218	245.6	0.051281	1750
15.84	115.5409	256	0.046833	1750
16.34	117.3839	266.6	0.042772	1750
16.84	119.1616	276.6	0.039064	1750
17.34	120.8925	284.2	0.035679	1750
17.84	122.6045	287.5	0.032588	1750
18.34	124.3371	284.4	0.029765	1750
18.84	126.1432	273.2	0.027188	1750
19.34	128.0918	253.6	0.024834	1750

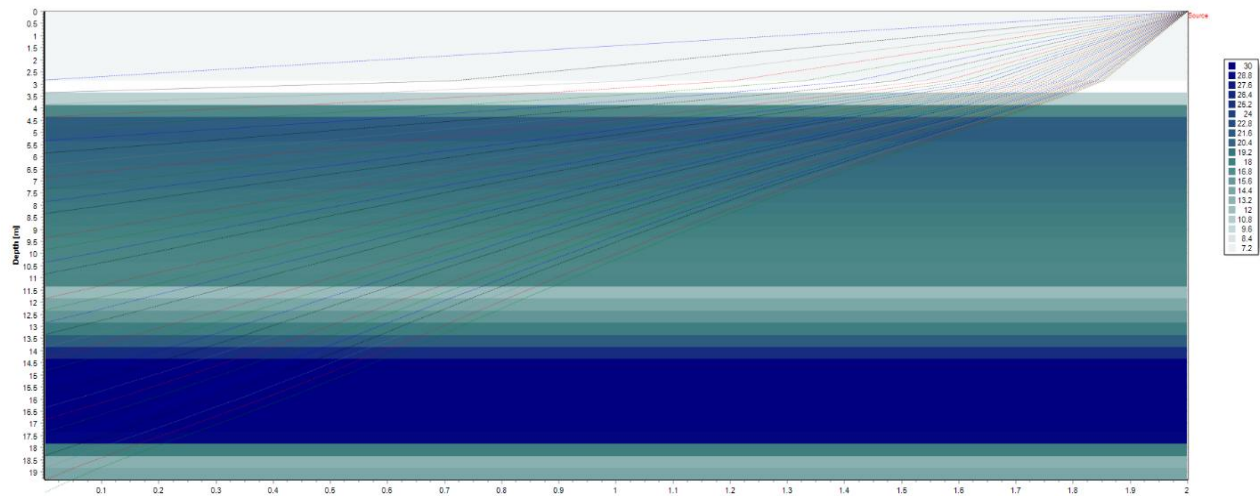


Figure 7. Estimated *FMDSMAA* absorption values after inputting the *DSTPolyKF*, *FMDSM* and *EKFAE* estimates outlined in Table 2.

Table 3. *FMDSMAA* output after inputting the estimates from the *DSTPolyKF*, *FMDSM* and *EKFAE* algorithms.

Depth [m]	Interval Velocity [m/s]	Absorption (α) [N_p/m]	Quality Factor (Q) [$1/N_p$]	Damping Ratio (η) [% N_p]	Wavelength (λ) [m]	Amplitude Ratio Residual
2.84	62.9	0.48854	6.87	7.28	0.79	N/A
3.34	126.5	0.29356	6.03	8.29	1.58	9.86E-07
3.84	149.4	0.14119	10.23	4.89	1.87	1.14E-06
4.34	162.4	0.07568	17.12	2.92	2.03	1.53E-07
4.84	168.5	0.06053	21.21	2.36	2.11	3.71E-07
5.34	171.2	0.06217	21.36	2.34	2.14	7.18E-07
5.84	172.5	0.06616	20.56	2.43	2.16	6.63E-07
6.34	173.6	0.06824	20.25	2.47	2.17	5.73E-07
6.84	174.9	0.06966	19.91	2.51	2.19	2.69E-07
7.34	176.5	0.07089	19.56	2.56	2.21	6.38E-07
7.84	178.3	0.07252	19.07	2.62	2.23	1.70E-06
8.34	180.4	0.07324	18.71	2.67	2.26	2.20E-06
8.84	182.6	0.07463	18.25	2.74	2.28	2.03E-06
9.34	184.9	0.07554	17.83	2.8	2.31	5.50E-07
9.84	187.3	0.07603	17.52	2.85	2.34	1.67E-06
10.34	189.9	0.07565	17.4	2.87	2.37	2.67E-07
10.84	192.6	0.07551	17.16	2.91	2.41	9.97E-07
11.34	195.7	0.07356	17.34	2.88	2.45	1.91E-06
11.84	199.2	0.10107	12.44	4.02	2.49	1.59E-07
12.34	203.2	0.08597	14.34	3.49	2.54	9.53E-07
12.84	207.8	0.07566	15.91	3.14	2.6	4.21E-07
13.34	213.3	0.06431	18.21	2.75	2.67	2.68E-05
13.84	219.8	0.05258	21.25	2.35	2.75	0.00017
14.34	227.3	0.04268	25.8	1.94	2.84	7.20E-05
14.84	235.9	0.03351	29.99	1.67	2.95	1.13E-03
15.34	245.6	0.02814	29.97	1.67	3.07	0.00474
15.84	256	0.02536	29.92	1.67	3.2	0.00726
16.34	266.6	0.02712	29.89	1.67	3.33	0.00864
16.84	276.6	0.0227	29.95	1.67	3.46	0.00847
17.34	284.2	0.02255	29.93	1.67	3.55	0.00549
17.84	287.5	0.02953	29.39	1.7	3.59	6.65E-06
18.34	284.4	0.04876	18.06	2.77	3.56	8.75E-06
18.84	273.2	0.06053	13.37	3.74	3.42	0.00283
19.34	253.6	0.06053	14.42	3.47	3.17	0.0175

Table 4. Field measurements of soil damping (after Stewart & Campanella, 1993)

Soil Type	Damping ratio η (% N_p)	Q [1/ N_p]
Sand	6	8.3
Silt	2.5	20
Alluvium (sand and clay)	12(<25m);3.5(>25m)	4.2(<25m);14.3(>25m)
Sandy	5	10
Clayey	1.7	29.4
Fine Sand	1.7	29.4
Bay mud	2.5	20
Clay	4-7	12.5-7.1
Sand (P-wave)	2-3	25-16.7

Erick Baziw

BCE's mission is to provide our clients around the world with state-of-the-art geotechnical signal processing systems, which allow for better and faster diagnostics of the sub-surface. Please visit our website (www.bcengineers.com) or contact our offices for additional information:

e-mail: info@bcengineers.com

phone: Canada: (604) 733 4995 – USA: (903) 216 5372